Available online at www.sciencedirect.com
SCIENCE DIRECT®
International Journal of Heat and Mass Transfer 47 (2004) 4547–4557
International Journal of HEAT and MASS TRANSFER
www.elsevier.com/locate/ijhmt

Pressure drop and heat transfer of arrays of in-line circular blocks on the wall of parallel channel

Tamotsu Igarashi *, Hajime Nakamura, Taketo Fukuoka

Department of Mechanical Engineering, National Defense Academy, 1-10-20 Hashirimizu, Yokosuka, Kanagawa 239-8686, Japan

Received in revised form 12 September 2003
Available online 11 June 2004

Abstract

Pressure drop and heat transfer of arrays of in-line circular blocks on the wall of a parallel channel are measured. Diameter and height of the blocks are 40 and 18 mm, respectively, while pitches of the blocks are varied. The effects of the number of lines and rows and other factors on pressure drop and heat transfer are investigated. The pressure loss coefficient ζ is the sum of the pressure drop across three regions, the inlet, intermediate and outlet regions, and is formulated as an empirical equation that agrees with experimental data to within ±10%. Average heat transfer coefficient of the first row of blocks is 10% lower than that of the second row. Coefficients of the first 5 rows Nu_{mi}, are approximated to within ±10% by $Nu_{mi} = 0.118(Re/\beta)^{0.75}$, where β is the opening ratio. The average Nusselt number of the second to fifth rows is also correlated to fan power, P_w, to within 5% by $Nu_{ave} = 190P_w^{0.25}$, where $P_w = \Delta P U_m A_0$, ΔP is the pressure difference, U_m is the mean velocity and A_0 is the cross-sectional area of the duct. Finally, the Nusselt number is represented by a non-dimensional expression as $Nu_{ave} = 0.134(\zeta^{1/3}Re)^{0.75}$.

Keywords: Pressure distribution; Pressure loss; Heat transfer; Forced convection; Circular blocks; In-line arrangement; Electric equipment; Fun power

1. Introduction

According to the design of air-cooled electronic equipment [1], pressure drop and heat transfer performance of the equipment are the most important factors. In previous papers [2–5], general correlations for pressure drop and heat transfer performance have not been presented. For example, Sparrow et al. [2,3] investigated on heat transfer of arrays of rectangular modules together with the measurement of pressure distributions on the duct wall. However, the value of the pressure drop was not quantitatively correlated to the heat transfer performance. The authors [6] have carried out experimental studies on the pressure loss across arrays of in-line square blocks having sizes similar to packages of electronic equipment on the wall of a parallel channel. Block heights, numbers of lines and rows, and pitches of the blocks were systematically varied. The pressure loss coefficient is given by the sum of the pressure drop across three regions: the inlet, intermediate and outlet ports.

In the present study, the pressure loss and average heat transfer of arrays of in-line circular blocks on the wall of a parallel channel were measured for various arrangements. The pressure loss coefficient is formulated by the same method as in a previous paper [4]. Average Nusselt numbers of the blocks are given by general equations, and agree with experimental data to within ±10%. Finally, average Nusselt number is correlated to the pressure loss coefficient and is given by a dimensionless expression. This fact enables the prediction of the pressure loss and average heat transfer of arrays of circular blocks.

* Corresponding author. Tel.: +81-46-841-3810; fax: +81-46-844-5900.
E-mail address: tigarash@nda.ac.jp (T. Igarashi).

0017-9310/$ - see front matter © 2004 Elsevier Ltd. All rights reserved.
doi:10.1016/j.ijheatmasstransfer.2003.09.038

Nomenclature

A	frontal area of blocks in a flow $= dHM$
A_0	cross-sectional area in a duct $= BW$
B, W	height and wide of a duct
Cp	pressure coefficient $= (p - p_a)/0.5\rho U_m^2$
Cp_1	pressure drop coefficient at inlet part $= (p_{upst} - p_1)/0.5\rho U_m^2$
Cp_2	pressure drop coefficient on array of blocks $= (p_1 - p_2)/0.5\rho U_m^2$
Cp_3	pressure raise coefficient at outlet part $= (p_{dnst} - p_2)/0.5\rho U_m^2$
d, H	diameter and height of a circular block
h_{mi}	average heat transfer coefficient of ith row block $= q/(\theta_{wi} - \theta_0)$
M, N	numbers of lines and rows
Nu_{ave}	mean Nusselt number per row $= \{\sum_{i=1}^{N} Nu_{mi}\}/N$ or $\{\sum_{i=2}^{N} Nu_{mi}\}/(N-1)$
Nu_{mi}	mean Nusselt number of ith rows $= h_{mi}d/\lambda$
P_w	fan power $= (p_{upst} - p_{dnst})Q$
p, p_a	pressure on a wall and atmospheric pressure
p_1, p_2	pressure at the inlet and outlet of array of blocks
P_1, P_2	pitches between array of blocks
Q	flow rate $= A_0 U_m = BWU_m$
Q_i	heat flow rate
q	heat flux $= Q_i/\pi(dH + d^2/4)$
Re	Reynolds number $= U_m d/v$
U_m	mean velocity at upstream
β	opening ratio $= 1 - A/A_0 = 1 - (B/H)(d/W)M$
δ	dominant factor $= (1 - \beta)/\beta^2$
ζ	pressure loss coefficient $= (p_{upst} - p_{dnst})/0.5\rho U_m^2$
λ	thermal conductivity of fluid
v, ρ	kinematic viscosity and density of fluid
θ_0, θ_{wi}	temperature of main flow and surface wall on the ith row block

Subscripts

exp, est experimental value and estimated value
upst, dnst upstream and downstream sides of blocks

2. Experimental apparatus and procedure

A schematic of the test section and symbols are shown in Fig. 1(a). The test section of height $B = 30$ mm, width $W = 250$ mm and length $L = 250$ mm was made of acrylic resin. Circular blocks of diameter $d = 40$ mm and height $H = 18$ mm were made of aluminium and positioned along the lower wall in an in-line arrangement. Both pitches of the blocks, P_1 and P_2, were individually varied from 50 to 80 mm. The number of lines M was varied from 5 to 3 and rows N varied from 5 to 2. Flow around the blocks was visualized by an oil-flow method at $U_m = 10$ m/s. The upper wall of the test section has many pressure taps of 0.6 mm in diameter in the flow direction at 10 mm interval and movable in the span direction. Pressure distribution on the upper wall was measured using an inclined manometer at $U_m = 10$ m/s. From the results of Matsushima et al. [5], the pressure drop is proportional to U_m^2, and therefore the pressure loss coefficient is independent of Reynolds number [6]. As shown in Fig. 1(b), the heat transfer model was made of copper block containing a heater, with six copper-constant thermocouples of 0.1 mm in diameter embedded in the surface. Four thermocouples were located on the side surface and two on the top surface. The heat transfer model was set up along the centerline of the test section, and the other blocks of the array were unheated. To clarify the effect of Reynolds number on Nusselt number, mean velocity U_m was set over a range from 2 to 10 m/s. The difference between the maximum and minimum temperatures of the six

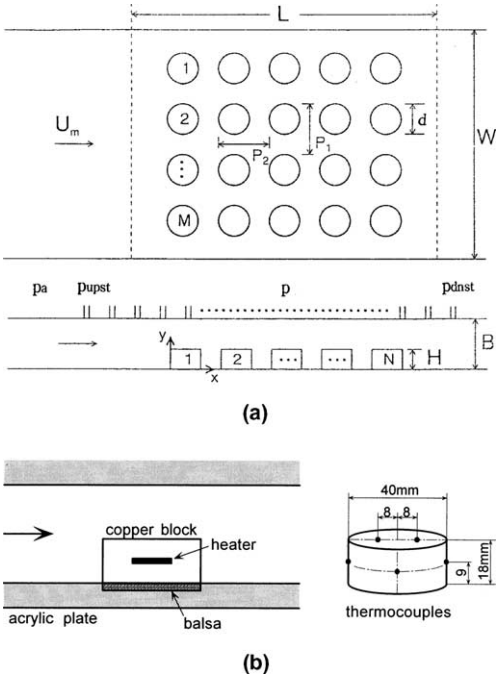

Fig. 1. Experimental apparatus: (a) configuration and symbols; (b) heat transfer model.

thermocouples in copper block of ith row was less than 1 °C. Mean surface temperature for ith row block was defined to be θ_{wi}. The average heat transfer coefficient of the block was obtained by $h_{mi} = q/(\theta_{wi} - \theta_0)$. Heat loss to the lower wall was about 1% of total heat flux.

3. Pressure drop

3.1. Flow around array of blocks

Fig. 2(a)–(c) show examples of surface oil-flow patterns on the blocks and base plate. In the case of $M = N = 3$, that is $P_1/d = P_2/d = 2$, horseshoe vortices are formed on the base plate around the blocks and a white crescent-shaped pattern appears on the first row of blocks, indicates the existence of a leading edge separation bubble. Large horseshoe vortices are formed on the base plate around the second row of blocks, but the crescent-shaped pattern disappears by the second row of blocks. Oil-flow patterns around the third row of blocks are similar to the second row of blocks. The separation point on the side surface of the block goes downstream near the top surface. In the case of $M = N = 4$, that is $P_1/d = P_2/d = 1.5$, imperfect horseshoe vortices are formed ahead of individual blocks from first to last row. For the case of $M = N = 5$, that is $P_1/d = P_2/d = 1.25$, imperfect horseshoe vortices are also formed ahead of individual blocks, with that of the second row larger than any of the other rows. This fact indicates that the heat transfer coefficient of the second row is higher than

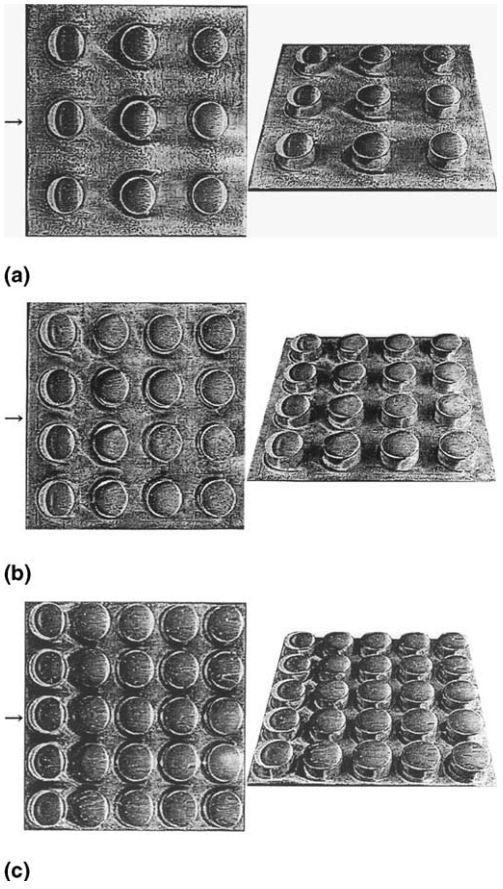

Fig. 2. Surface oil-flow patterns: $d = 40$ mm, $H = 18$ mm, $U_m = 10$ m/s. (a) $P_1/d = P_2/d = 2.0$; (b) $P_1/d = P_2/d = 1.5$; (c) $P_1/d = P_2/d = 1.25$.

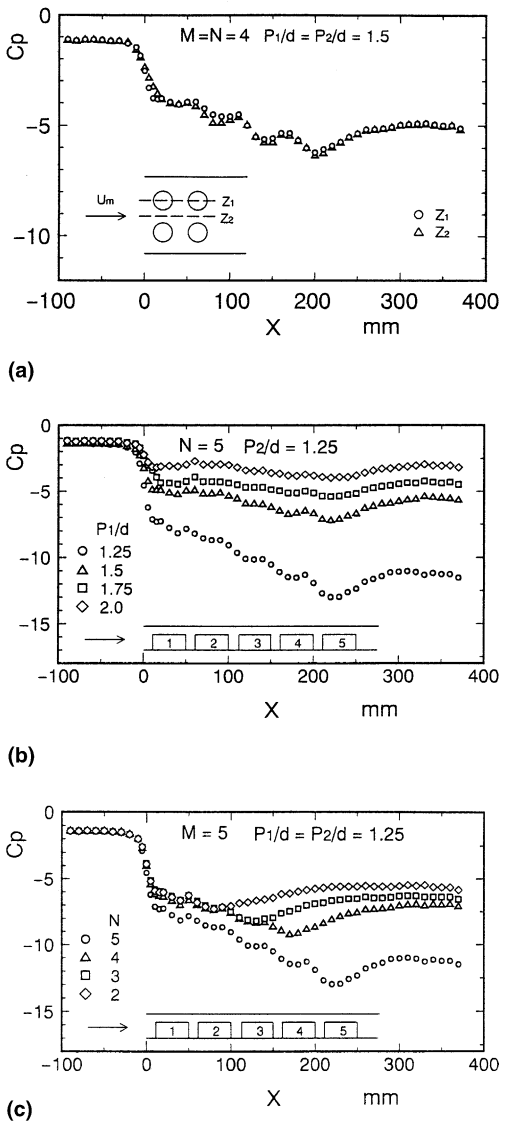

Fig. 3. Pressure distributions: (a) effect of tap position; (b) effect of pitch P_1; (c) effect of number N.

the first row. Moreover, downwash [7] from the top face to downstream of the side faces of the circular blocks is not observed.

3.2. Pressure distribution and pressure loss coefficient

The effect of pitch P_1 on the pressure distribution on the upper wall is shown in Fig. 3(a)–(c). Pressure coefficient at inlet of the first row of blocks decreases suddenly by vena contracta, with the pressure drop becoming remarkably large as P_1 decreases. Pressure coefficient decreases gradually along the downstream blocks, and then recovers at the outlet of the blocks. Formulation of the pressure loss coefficient ζ is attempted in the same manner as in a previous report [6]. As shown in Fig. 4, the pressure loss coefficient is divided into three localized pressure coefficients, at the

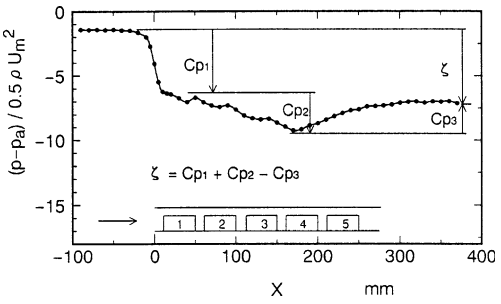

Fig. 4. Division of pressure drop.

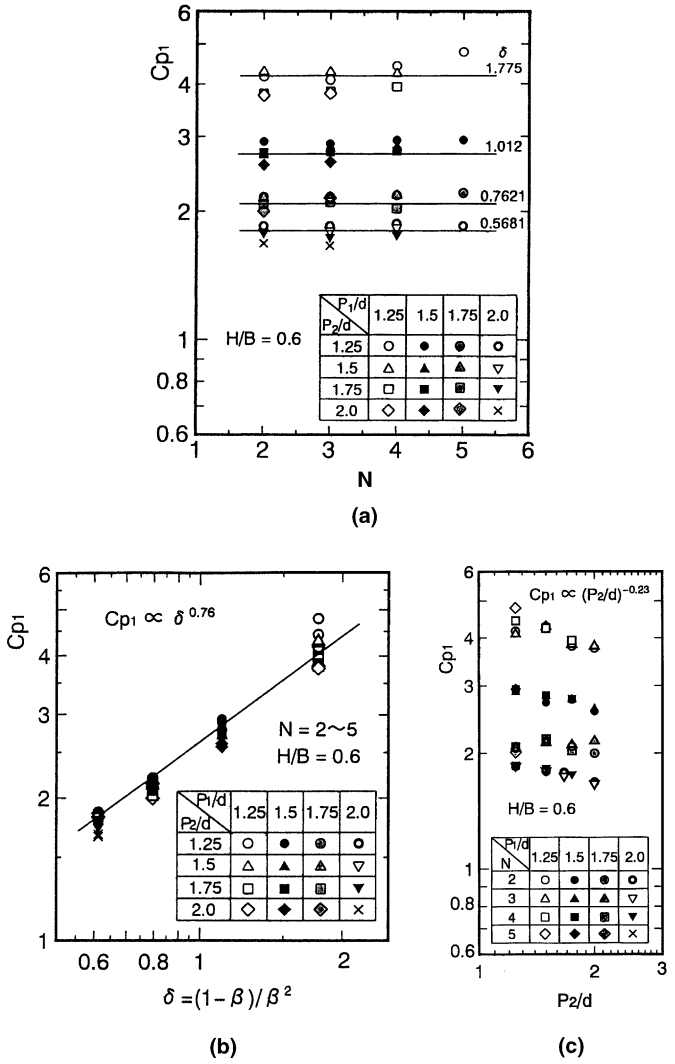

Fig. 5. Pressure drop at inlet: (a) Cp_1 vs N; (b) Cp_1 vs δ; (c) Cp_1 vs P_2/d.

inlet of the first block, Cp_1, between first and last blocks, Cp_2, and downstream of the last block, Cp_3.

$$\zeta = (p_{upst} - p_{dnst})/0.5\rho U_m^2 = [(p_{upst} - p_1) + (p_1 - p_2) + (p_2 - p_{dust})]/0.5\rho U_m^2 \quad (1)$$

$$\zeta = Cp_1 + Cp_2 - Cp_3 \quad (2)$$

The above three coefficients are represented using the following dimensionless dominant factors.

$$Cp_1, Cp_2, Cp_3 = f(H/d, H/B, W/d, P_1/d, P_2/d, M, N) \quad (3.1)$$

The opening ratio $\beta = 1 - (Hd/BW)M$ and the dominant factor $\delta = (1-\beta)/\beta^2$ obtained in the hydraulic losses of flow control devices are introduced [8,9]. Eq. (3.1) can be rewritten as

$$Cp_1, Cp_2, Cp_3 = f(\delta, P_1/d, P_2/d, N) \quad (3.2)$$

3.3. Formulation of pressure drop coefficient

3.3.1. Pressure drop at inlet

The effects of N, δ and P_2/d on Cp_1 are shown in Fig. 5(a)–(c). The effect of N is neglected and factor δ is expressed as $Cp_1 \propto \delta^{0.76}$. The value of Cp_1 decreases slightly with an increase in P_2/d and can be expressed by $Cp_1 \propto (P_2/d)^{-0.23}$, leading to the following equation:

$$Cp_1 = 2.86\delta^{0.76}(P_2/d)^{-0.23} \quad (4)$$

3.3.2. Pressure increase at outlet

Fig. 6(a)–(c) show the effects of N, δ and P_2/d on the pressure rise coefficient at the outlet, Cp_3. The effect of N on Cp_3 cannot be disregarded and is given by $Cp_3 \propto (N-1)^{0.09}$, and the effects of δ and P_2 are given by $Cp_3 \propto \delta^{0.47}$ and $Cp_3 \propto (P_2/d)^{-0.18}$. The constant value defined by $Cp_3/\{\delta^{0.47}[(N-1)/(P_2/d)^2]^{0.09}\}$ averaged over all data is nearly 1.13, leading to the following equation:

$$Cp_3 = 1.13\delta^{0.47}[(N-1)/(P_2/d)^2]^{0.09} \quad (5)$$

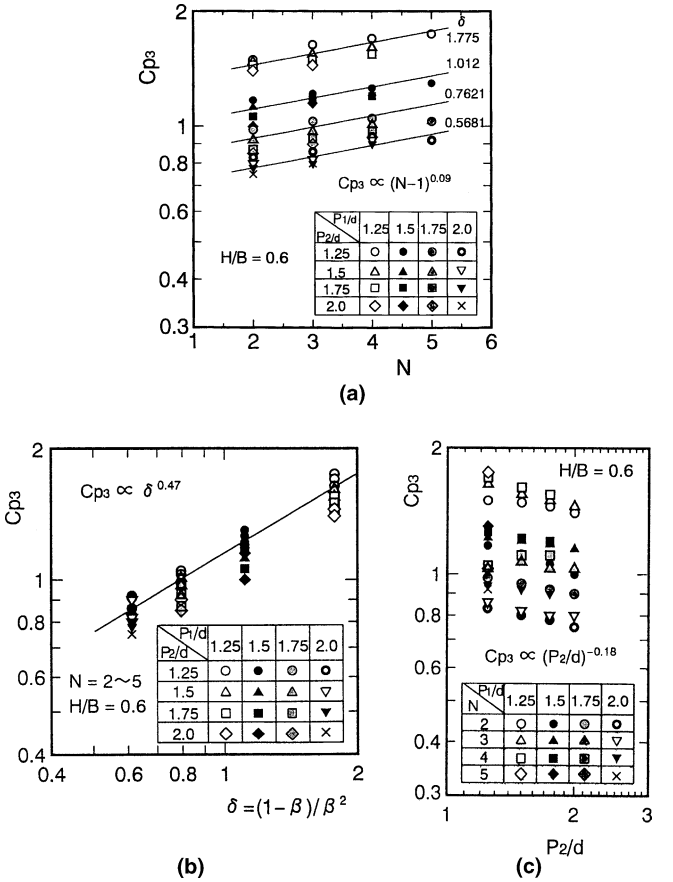

Fig. 6. Pressure rise at outlet: (a) Cp_3 vs N; (b) Cp_3 vs δ; (c) Cp_3 vs P_2/d.

3.3.3. Pressure drop between inlet and outlet

The effects of N, δ and P_2/d on the pressure drop coefficient between inlet and outlet parts, Cp_2 are shown in Fig. 7(a) and (b). By expressing the effects of N and P_2/d by the function $[(N-1)(P_2/d-1)]$, the correlation $Cp_2 \propto [(N-1)(P_2/d-1)]^{0.47}$ is obtained. The effect of δ is $Cp_2 \propto \delta^{0.86}$. By neglecting the effect of P_1/d on Cp_2, the constant value defined by $Cp_2/\{\delta^{0.86}[(N-1)\times(P_2/d-1)]^{0.47}\}$ averaged over all data is 1.40, leading to the following equation:

$$Cp_2 = 1.40\delta^{0.86}[(N-1)/(P_2/d-1)]^{0.47} \quad (6)$$

3.4. Estimation equation for pressure drop coefficients

Pressure drop coefficients and pressure rise coefficient of the three sections are given by Eqs. (4)–(6). Individual estimated values obtained by the above equations agree well with experimental values within ±10%, as shown in Fig. 8(a)–(c). Thus, the estimated pressure loss coefficient of the array of blocks, ζ_{est}, can be obtained by substituting Eqs. (4)–(6) into Eq. (2). As shown in Fig. 9, estimated values, ζ_{est} agree well with the experimental values, ζ_{exp}, within ±10%.

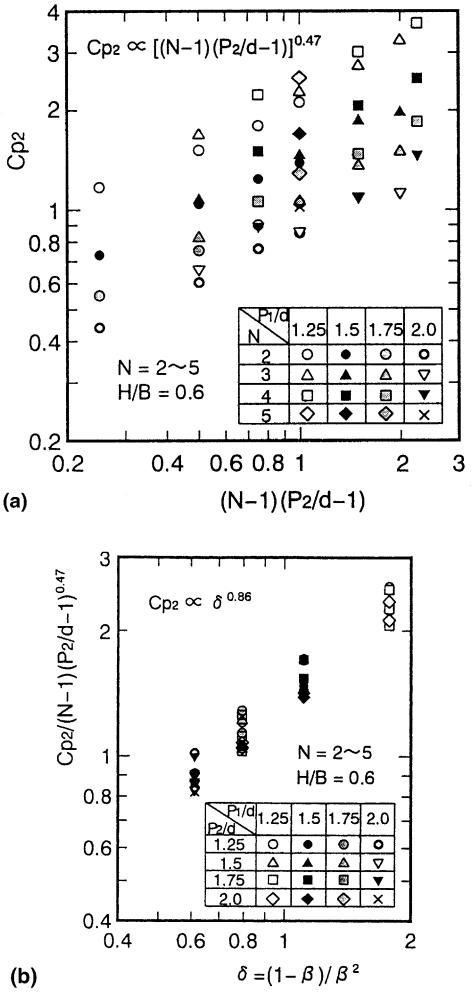

Fig. 7. Pressure drop between inlet and outlet: (a) Cp_2 vs $(N-1)(P_2/d-1)$; (b) $Cp_2/\{(N-1)(P_2/d-1)\}$ vs δ.

4. Heat transfer characteristics

4.1. Average heat transfer of arrays of circular blocks

The average heat transfer of a single circular block and that of an array of in-line blocks for the cases $M = N = 3$, $P_1/d = P_2/d = 2.0$ and $M = 3$, $N = 5$, $P_1/d = 2.0$, $P_2/d = 1.25$ are shown in Fig. 10(a) and (b), respectively. The average Nusselt number of single block is given by

$$Nu_m = 0.13Re^{0.75} \quad \text{(single block)} \quad (7)$$

where, $Nu_m = h_m d/\lambda$, $Re = U_m d/v$. The two broken lines in Fig. 10(a) correspond to those of a single circular block having $d = 80$ mm and $H = 28$ mm in laminar and turbulent boundary layers [5].

$$Nu_{mL} = 0.38Re^{0.62} \quad (\delta_L/H = 0.06 \sim 0.13) \quad (8.1)$$

$$Nu_{mT} = 0.42Re^{0.62} \quad (\delta_T/H = 0.52 \sim 1.52) \quad (8.2)$$

where δ_L and δ_T are the thicknesses of laminar and turbulent boundary layers. The Nusselt number of the present experiment is slightly higher than that in a turbulent boundary layer. For the case of $M = 3$, $N = 3$–5, the Nusselt number of ith row block, Nu_{mi}, can be approximately expressed by

$$Nu_{mi} = 0.15Re^{0.75} \quad (P_1/d = 2.0,\ P_2/d = 2.0 \sim 1.25,\ i = 1\text{–}5) \quad (9)$$

Fig. 11(a) and (b) show examples of $M = 4$, $P_1/d = P_2/d = 1.50$ for $N = 3$ and 5, respectively. The Nusselt number of the first row of blocks is 15% lower than downstream. At the downstream blocks, there are no significant differences in number of rows N. These Nusselt numbers of ith row block can be given approximately by

$$Nu_{m1} = 0.16Re^{0.75} \quad (P_1/d = P_2/d = 1.5,\ N = 3\text{–}5) \quad (10.1)$$

$$Nu_{mi} = 0.18Re^{0.75} \quad (P_1/d = P_2/d = 1.5,\ N = 3\text{–}5,\ i = 2\text{–}5) \quad (10.2)$$

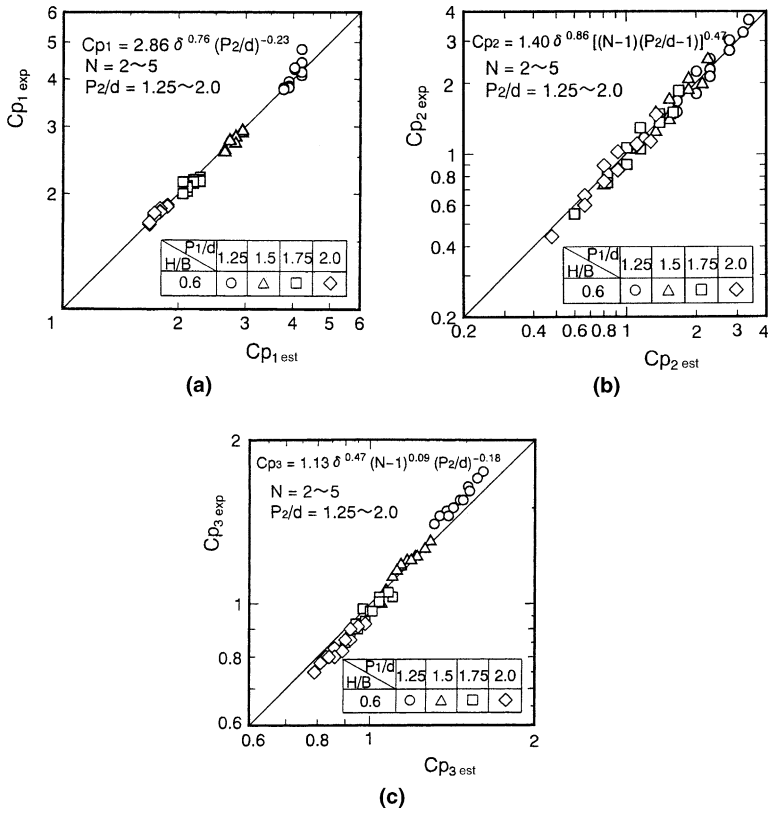

Fig. 8. Empirical values vs experimental values: (a) Cp_1; (b) Cp_2; (c) Cp_3.

Fig. 11(c) and (d) show examples of $M = 5$, $P_1/d = P_2/d = 1.25$ for $N = 3$ and 5, respectively. For $N = 3$, there is no difference between the Nusselt number of the first row of blocks and those of downstream blocks. For $N = 5$, these Nusselt numbers are lower than for $N = 3$, and values at downstream blocks are slightly higher than at upstream blocks. Nusselt numbers of the ith row block can be approximately be given by

$$Nu_{mi} = (0.16 \sim 0.19)Re^{0.75} \quad (P_1/d = P_2/d = 1.25,\ N = 3\text{–}5,\ i = 1\text{–}5) \tag{11}$$

In all cases of block arrangement, Nusselt numbers of individual blocks are proportional to $Re^{0.75}$, and increase with increasing M, that is, pitch P_1/d. This is caused by an increase in flow velocity around the blocks due to the high blockage effect on the flow path. Formulation of the Nusselt number considering the blockage effect is attempted. Introducing the opening ratio β, the modified Reynolds number is defined by $Re^* = Re/\beta$. For the cases of $M = N = 3, 4$ and 5, the Nusselt numbers are rearranged by Re^*, and are shown in Fig. 12. For single and ith row blocks in array, all experimental data is approximately expressed within ±10% as follows:

$$Nu_{mi} = 0.118(Re^{0.75}) \quad (i = 1\text{–}5,\ \beta = 0.52\text{–}0.90) \tag{12}$$

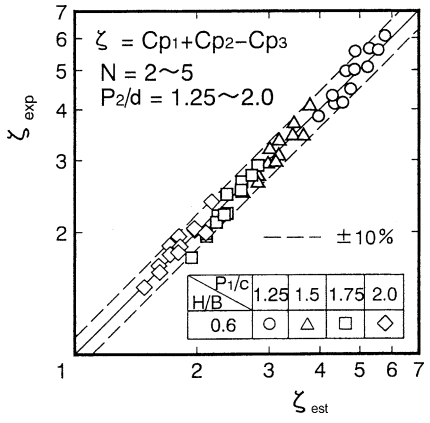

Fig. 9. Pressure loss coefficient ζ.

4.2. Correlation between heat transfer and pressure loss

Fan (pumping) power, P_w, is an important factor in performance assessment, and is defined as

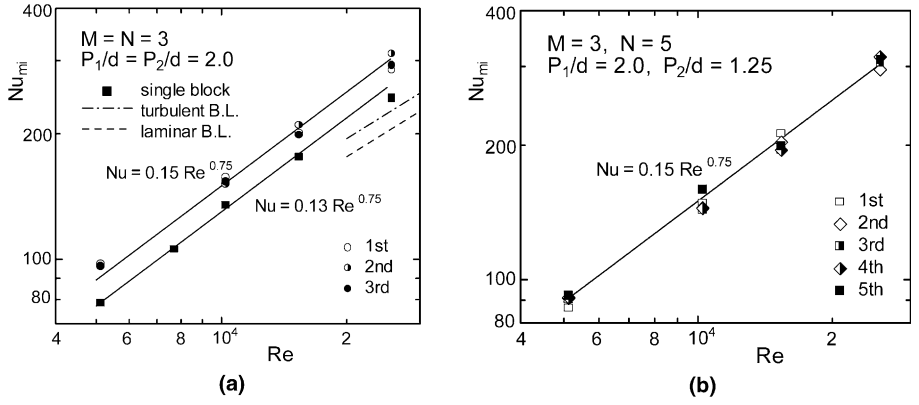

Fig. 10. Mean Nusselt number ($M = 3$): (a) $M = N = 3, P_1/d = P_2/d = 2.0$; (b) $M = 3 = N = 5, P_1/d = 2.0, P_2/d = 1.25$.

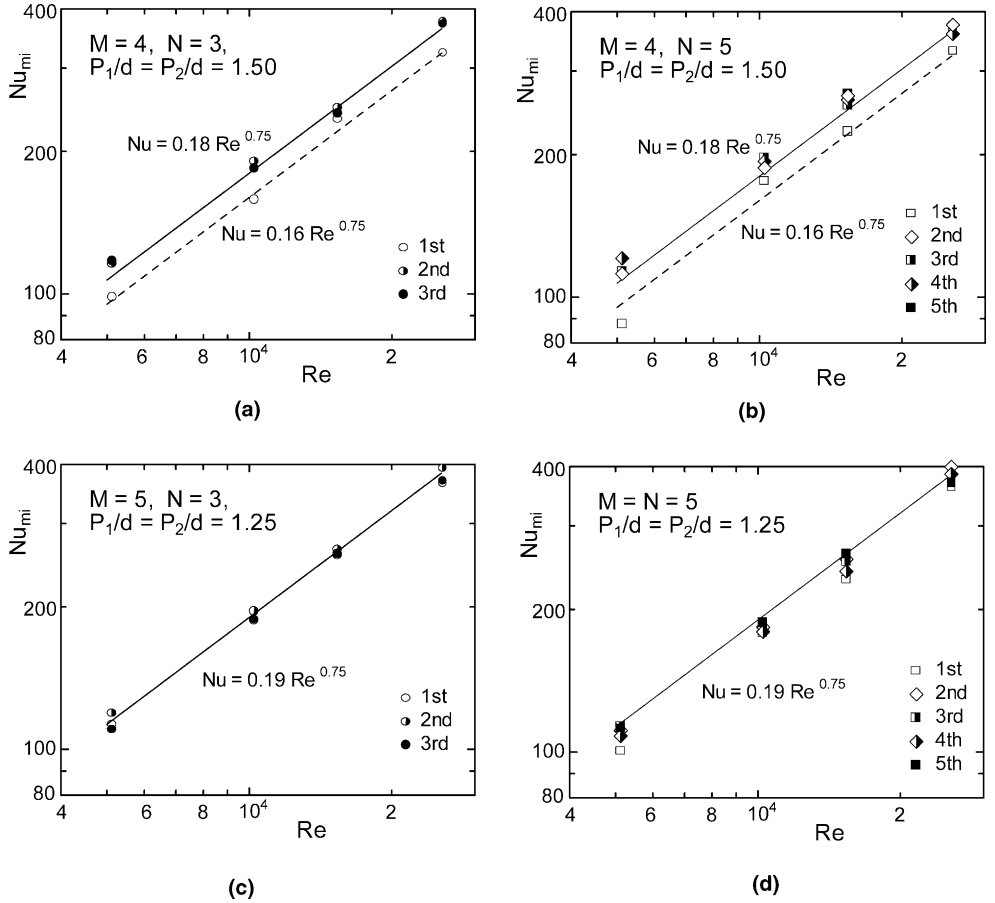

Fig. 11. Mean Nusselt number ($M = 4, 5$): (a) $M = 4, N = 3, P_1/d = P_2/d = 1.5$; (b) $M = 4, N = 5, P_1/d = P_2/d = 1.5$; (c) $M = 5, N = 3, P_1/d = P_2/d = 1.25$; (d) $M = N = 5, P_1/d = P_2/d = 1/25$.

$$P_w = \Delta p \cdot Q = \Delta p \cdot BW \cdot U_m \quad [W] \tag{13}$$

where $BW \cdot U_m$ is the flow rate Q, and Δp is the pressure drop, $(p_{upst} - p_{dnst})$, between the inlet and outlet of the array of blocks. Δp can be measured, or calculated from the following equation:

$$\Delta p = \zeta 0.5 \rho U_m^2 \tag{14}$$

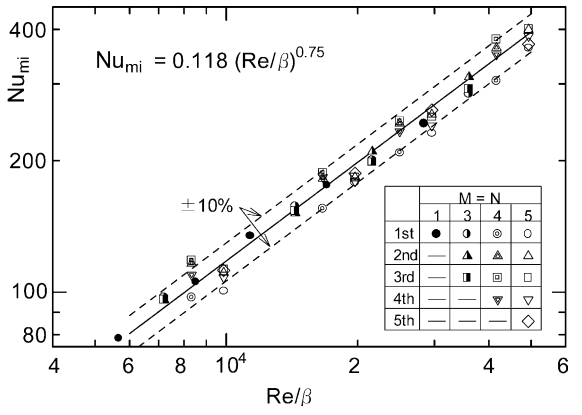

Fig. 12. Mean Nusselt number arranged by modified Reynolds number.

Total heat flow rate Nu_{total} of arrays of in-line blocks is given by the sum of $Nu_{\text{m}i}$

$$Nu_{\text{total}} = M \sum_{i=1}^{N} Nu_{\text{m}i} \tag{15}$$

Average Nusselt number per block, Nu_{ave}, is given by Nu_{total}/MN. The correlation between fan power P_{w} and total Nusselt number Nu_{total} is shown in Fig. 13 for cases of $M = 3, 4, 5$ and $N = 3, 4, 5$. Fan power P_{w} is proportional to the number of blocks and total Nusselt number is also proportional to $P_{\text{w}}^{1/4}$. Average Nusselt number per block Nu_{ave} is related to fan power as follows:

$$Nu_{\text{ave}} = Nu_{\text{total}}/MN = 185P_{\text{w}}^{1/4} \quad [\text{W}] \tag{16}$$

This equation agrees well with experimental values to within ±5%. From Eqs. (13) and (14), fan power P_{w} is proportional to U_{m}^3, and the dependency of mean

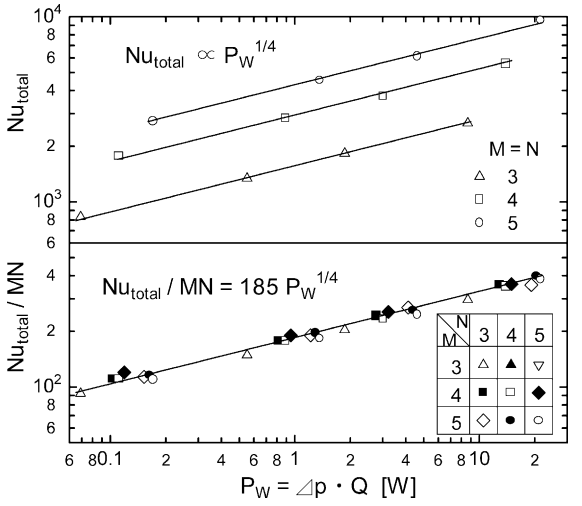

Fig. 13. Total Nusselt number vs fan power.

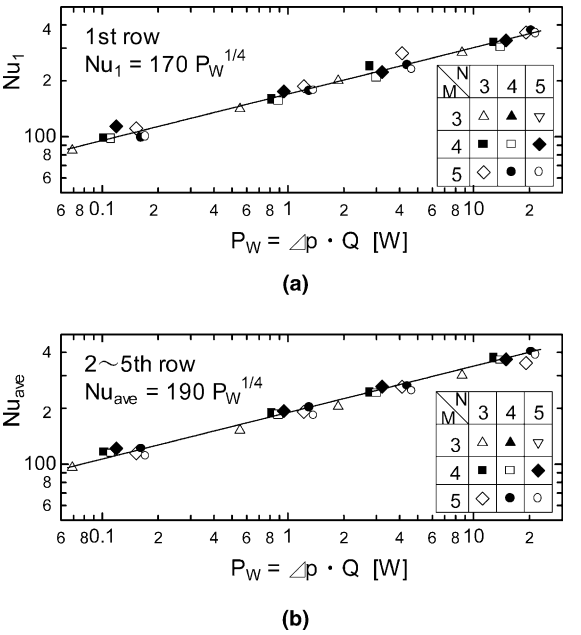

Fig. 14. Average Nusselt number vs fan power: (a) first row; (b) second to fifth rows.

velocity U_{m} on Nusselt number is $Nu_{\text{ave}} \propto U_{\text{m}}^{3/4}$, resulting in the dependency of Reynolds number on the Nusselt number to be $Nu_{\text{ave}} \propto Re^{3/4}$. This exponent 0.75 coincide with those of Eqs. (9)–(11) in the previous section. From Eq. (16), high density arrays exhibit good heat transfer performance in the range of the present opening ratio of $\beta = 0.52$–0.72. From the facts described above, the total Nusselt number Nu_{total} and average Nusselt number Nu_{ave} can be concluded to have been obtained from experimental conditions. That is, the fan power P_{w} in Eq. (16) is obtained from Eqs. (13) and (14), and the pressure loss coefficient, ζ, is obtained from Eqs. (4)–(6). In the previous section, the Nusselt number of the first row is lower than the downstream rows. The correlation between average Nusselt number Nu_{ave} of ith row of blocks in the array and fan power of the array is shown in Fig. 14(a) and (b), giving the following correlation equations:

$$Nu_1 = 170P_{\text{w}}^{0.25} \quad (i = 1) \tag{17.1}$$

$$Nu_{\text{ave}} = 190P_{\text{w}}^{0.25} \quad (i = 2\text{–}5) \tag{17.2}$$

In Eqs. (16), (17.1) and (17.2), the left side Nusselt number Nu is non-dimensional, but the right side term P_{w} is power (units of Watts).

4.3. Dimensionless correlation equation

As the dimensions on the left and right sides of Eqs. (17.1) and (17.2) are not equal, an attempt to obtain

dimensionless correlation equations from dimensional analysis is made. Physical quantities concerning the heat transfer phenomena are:

$$h_m = f(U_m, d, H, P_1, P_2, B, W, \mu, \rho, Cp, \lambda) \tag{18}$$

where μ, ρ, Cp and λ are physical properties of the fluid and the parameters H, P_1, P_2, B and W are included in the pressure difference Δp, and are thus replaced by Δp to give

$$h_m = f(U_m, d, \Delta p, \mu, \rho, Cp, \lambda) \tag{19}$$

Dimensional analysis leads us to the next correlation.

$$h_m d/\lambda = f[\Delta p/\rho U_m^2, U_m d/(\mu/\rho), \mu Cp/\lambda) \tag{20}$$

The above four dimensionless groups are Nu_m, ζ, Re and Prandtl number Pr, respectively.

$$Nu_m = f(\zeta, Re, Pr) \tag{21}$$

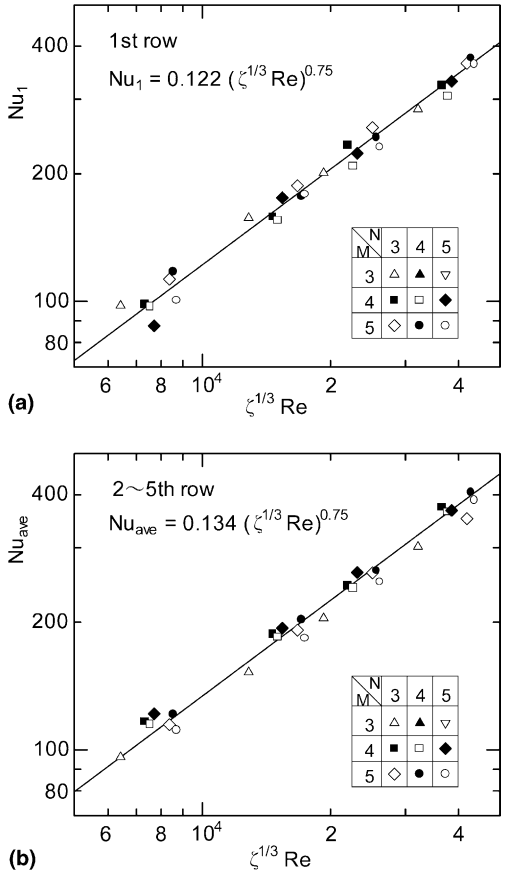

Fig. 15. Dimensionless expression: (a) first row; (b) second to fifth rows.

In this case, the Prandtl number of air is nearly constant, leading to the following equation:

$$Nu_m = f(\zeta, Re) = C\zeta^m Re^n \tag{22}$$

Eq. (16) and Eqs. (13), (14) are used to determine the exponents of the above equation, $m = 0.25$ and $n = 0.75$. Then Eq. (22) can be rearranged to give:

$$Nu_m = C(\zeta^{1/3} Re)^{0.75} \tag{23}$$

The above correlations for all experimental data are shown in Fig. 15(a) and (b). Average Nusselt numbers of first row and second to fifth rows of blocks are given by the following dimensionless expressions:

$$Nu_1 = 0.122(\zeta^{1/3} Re)^{0.75} \quad (i = 1) \tag{24}$$

$$Nu_1 = 0.134(\zeta^{1/3} Re)^{0.75} \quad (i = 2\text{–}5) \tag{25}$$

The above equations agree well with experimental data to within ±5%. Moreover, errors in the Nusselt number of the ith row $Nu_{mi}(i = 2\text{–}5)$ and average Nusselt number of row Nu_{ave} are $(Nu_{mi} - Nu_{ave})/Nu_{ave} < \pm 0.02$ for all experimental data.

5. Conclusions

The results lead to the following conclusions:

(1) Total pressure loss coefficient ζ, can be expressed as the sum of pressure drop coefficients at the inlet and intermediate sections of the array, Cp_1, Cp_2 and the pressure rise at the outlet of the array Cp_3:

$$\zeta = Cp_1 + Cp_2 - Cp_3$$

Individual coefficients are given as follows:

$$Cp_1 = 2.86\delta^{0.76}(P_2/d)^{-0.23};$$
$$Cp_2 = 1.40\delta^{0.86}[(N-1)(P_2/d-1)]^{0.47};$$
$$Cp_3 = 1.13\delta^{0.47}[(N-1)(P_2/d)^2]^{0.09}$$

(2) Average heat transfer of the first row is lower by about 10% than those of the second to fifth rows. As M increases, heat transfer increases due to the blockage effect.

(3) Average heat transfer of ith row of blocks can be expressed by the following equation using the opening ratio β.

$$Nu_{mi} = 0.118(Re/\beta)^{0.75} \quad (i = 1\text{–}5,\ \beta = 0.52\text{–}0.90)$$

(4) The correlation between average Nusselt number and fan (pumping) power is given by

$$Nu_1 = 170(P_w)^{0.25} \quad (P_w : [\mathrm{W}]),$$

$$Nu_{ave} = 190(P_w)^{0.25} \quad (i = 2\text{–}5)$$

(5) Introducing the pressure loss coefficient, ζ, the above equations can be rewritten as dimensionless expressions:

$$Nu_1 = 0.122(\zeta^{1/3}Re)^{0.75},$$

$$Nu_{ave} = 0.134(\zeta^{1/3}Re)^{0.75} \quad (i = 2\text{–}5)$$

(6) In the range of the present blockage ratio, a high-density array successfully produces good heat transfer performance.

Acknowledgements

The authors wish to thank Mr. T. Hiraoka of the former student of National Defense Academy for his assistance in the heat transfer experiments.

References

[1] JSME Handbook on Cooling Design of Electronic Equipment, 1995 (in Japanese).
[2] E.M. Sparrow, J.E. Niethammer, A. Chaboki, Heat transfer and pressure drop characteristics of arrays of rectangular modules encountered in electronic equipment, Int. J. Heat Mass Transfer 25 (7) (1982) 961–973.
[3] E.M. Sparrow, S.B. Vemuri, D.S. Kadle, Enhanced and local heat transfer, pressure drop, and flow visualization for arrays of block-like electronic components, Int. J. Heat Mass Transfer 26 (5) (1983) 689–699.
[4] R.T. Moffat, D.E. Arvizu, A. Ortega, Cooling electronic components: forced convection experiments with an air-cooled array, Heat Transfer Equipment, HTD, vol. 48, ASME/AIChE, Annual Heat Transfer Conference, 1985, pp. 17–27.
[5] H. Matsushima, T. Yanagida, W. Nakayama, Pressure drop characteristics of circuit board with arrays of LSI package, Trans. Jpn. Soc. Mech. Eng. 59 (560B) (1993) 1244–1251.
[6] T. Igarashi, T. Fukuoka, Pressure drop of arrays of in-line blocks on the wall of parallel channel, Trans. Jpn. Soc. Mech. Eng. 66 (646B) (2000) 1535–1543.
[7] T. Tsutsui, T. Igarashi, H. Nakamura, Fluid flow and heat transfer around a cylindrical protuberance mounted in a flat plate boundary layer, Trans. Jpn. Soc. Mech. Eng. 65 (633B) (1999) 1716–1723, or;
T. Tsutsui, T. Igarashi, H. Nakamura, JSME Int. J. 43 (2B) (2000) 279–287.
[8] T. Igarashi, Flow Resistance of a vortex shedder in a circular pipe, in: Proc. of Fifth Triennial Int. Symp. on Fluid Control, Measurement and Visualization, Hayama, 1997, pp. 743–748.
[9] T. Igarashi, Hydraulic losses of flow control devices in pipes, JSME Int. J. 38 (3B) (1995) 398–403.